PHYSICAL REVIEW B **95**, 060506(R) (2017)

Topological surface superconductivity in doped Weyl loop materials

Yuxuan Wang[1] and Rahul M. Nandkishore[2]

[1]*Department of Physics and Institute for Condensed Matter Theory, University of Illinois at Urbana-Champaign, Urbana, Illinois 61801, USA*

[2]*Department of Physics and Center for Theory of Quantum Matter, University of Colorado, Boulder, Colorado 80309, USA*

(Received 27 October 2016; published 27 February 2017)

We study surface superconductivity involving the "drumhead" surface states of (doped) Weyl loop materials. The leading weak-coupling instability in the bulk is toward a chiral superconducting order, which fully gaps the Fermi surface. In this state the surface also becomes superconducting, with $p + ip$ symmetry. We show that the surface SC state is "topological" as long as it is fully gapped, and the system traps Majorana modes wherever a vortex line enters or exits the bulk. In contrast to true two-dimensional $p + ip$ superconductors, these Majorana zero modes arise even in the "strong pairing" regime where the chemical potential is entirely above/below the drumhead. We also consider conventional s-wave pairing, and show that in this case the surface hosts a flat band of charge neutral Majorana fermions, whose momentum range is given by the projection of the bulk Fermi surface. Weyl loop materials thus provide access to new forms of topological superconductivity.

DOI: 10.1103/PhysRevB.95.060506

Nodal-line semimetals are a new class of topological materials that has recently been proposed [1–9] and observed in Ca_3P_2 [10], $TlTaSe_2$ [11], CaAgP, and CaAgAs [12]. A Weyl loop material is the simplest example of these systems which at a particular filling display a twofold degenerate one-dimensional (1D) Fermi ring in the bulk (which becomes toroidal upon doping), with massless Dirac-like quasiparticles. These materials constitute a new class of electronic system that is intermediate between Weyl semimetals (where the Fermi surface is pointlike), and ordinary three-dimensional metals (with a two-dimensional Fermi surface). As such, they can support a qualitatively new phenomenology which is arousing considerable interest [5,13,14].

While most research on Weyl loop materials has focused on the *noninteracting* materials, these systems also provide a new playground for investigating the *correlated states* that may arise through weak-coupling instabilities. For example, Ref. [15] used general symmetry arguments to establish that Weyl loop materials are natural candidates to host exotic forms of superconductivity (SC) in the bulk, with the leading weak-coupling instability being to a fully gapped chiral superconducting state in three dimensions, which has never before been observed. This conclusion was also borne out by detailed microscopic calculations within a renormalization group formalism in Ref. [16]. Separately, it has been pointed out that Weyl loop materials host "drumhead" surface states [17] (see also Refs. [18–20]) with a a large density of states, which could naturally support high temperature surface SC [21]. However, a detailed analysis of the symmetry and topology of surface superconductivity in these materials has yet to be performed [22].

In this Rapid Communication we provide a systematic analysis of the symmetry and topology structure of surface superconductivity in Weyl loop materials, as well as its interplay with bulk superconductivity and the superconducting proximity effect. We begin by reviewing the structure of bulk SC before turning to surface SC. We discuss "conventional" s-wave states, and show that the surface state is immune to a proximity effect from the s-wave order. However, bulk s-wave pairing induces gapless surface SC, with a new drumhead of surface states made out of charge-neutral Majorana fermions. We then discuss surface SC in the presence of bulk chiral p-wave superconductivity, which is [15,16] the only fully gapped bulk state. In this case we show that the surface develops $p + ip$ chiral superconducting order, and is fully gapped, except for some special cases where the drumhead band is at zero energy at a time-reversal invariant (TRI) momentum. In analogy with the two-dimensional (2D) $p + ip$ superconductor [23,24], it is tempting to classify the surface SC with a Fermi surface (FS) of the drumhead band as topological and the opposite case as topologically trivial. However, we show that this is not the case—as long as the surface SC is gapped, it is *topological* and traps Majorana zero modes (MZMs) where a vortex line enters or exits the bulk. Here, the distinction with 2D $p + ip$ SC arises because the drumhead band does not cover the full 2D Brillouin zone (BZ). We establish this by means of analytic arguments based on adiabatic continuation, and also verify this numerically. Weyl loop materials thus provide access to new forms of topological (surface) superconductivity, distinct from previous proposals (e.g., Ref. [25]).

Model. We consider a two-band model,

$$\mathcal{H}(\mathbf{k}) = \sigma^x(6 - t_1 - 2\cos k_x - 2\cos k_y - 2\cos k_z) + 2t_2\sigma^y \sin(k_z) - \mu, \tag{1}$$

where we have factored out an overall energy scale, and the matrices σ^x and σ^y (hereafter "spin") can either be in SU(2) spin space, or simply in a two-band subspace of a multiband system. For small $t_{1,2}$ the first two terms describe a line node in the dispersion, given by $2 - t_1/2 - \cos k_x - \cos k_y = 0$ and $k_z = 0$. The last term is a chemical potential that gives rise to a nondegenerate Fermi surface surrounding the nodal line, which forms a torus. The dispersion in the continuum limit can be written as $\mathcal{H} = \sigma^x(k_\parallel^2 - t_1) + 2t_2\sigma^y k_z - \mu$, where $k_\parallel^2 = k_x^2 + k_y^2$. At a given polar angle θ (defined by $k_y/k_x = \tan\theta$), for a small μ, the cross section of the FS is given by two ellipses at $t_1(k_\parallel \pm \sqrt{t_1})^2 + t_2 k_z^2 = \mu^2$. Without loss of generality we set $t_1 = t_2$ and parametrize this circle by another angle φ, as shown in Fig. 1, such that the linearized Hamiltonian takes the form $H = K(\cos\varphi\sigma^x + \sin\varphi\sigma^y)$, where $K\cos\varphi = k_\parallel - \sqrt{t_1}$

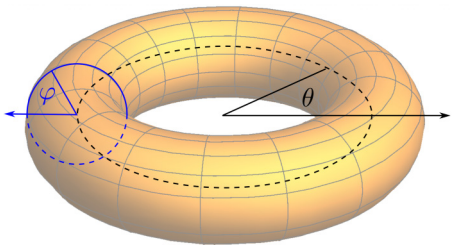

FIG. 1. The torus-shaped Fermi surface of a Weyl loop metal.

and $K \sin\varphi = t_1 k_z$. Note that inversion takes $\theta \to \theta + \pi$ and $\varphi \to -\varphi$ with this parametrization.

Superconductivity in the bulk. We first consider the superconducting order parameter in the odd-parity channels that couples to fermions via

$$H^o_\Delta = \Delta \psi^\dagger(\mathbf{k})[\mathbf{d}(\mathbf{k})\cdot\boldsymbol{\sigma}] i\sigma^y (\psi^\dagger)^T(-\mathbf{k}). \tag{2}$$

Fermionic statistics require $\mathbf{d}(\mathbf{k})$ to be odd in $\mathbf{k}$. From the torus configuration of the FS, we expect that energetically the leading SC instability is toward an order parameter with $\mathbf{d}(\mathbf{k}) \propto e^{i\theta}\tilde{\mathbf{d}}(\mathbf{k})$, where $\tilde{\mathbf{d}}(\mathbf{k})$ is an even function. We focus on the cases where $\tilde{\mathbf{d}}(\mathbf{k})$ is a constant on the FS, and is pointed toward the x, y, or z directions. Because of the nontrivial spin texture, the SC order parameter projects onto the low energy fermions with nontrivial "projective form factors" [26]. To this end, we note that the spinor structure of a low energy fermion (conduction band) on the FS is given by $c^\dagger(\mathbf{k}) = \sum_{\alpha=\uparrow,\downarrow} \xi_\alpha \psi^\dagger_\alpha(\mathbf{k})$, where $\xi = [\exp(i\varphi/2), \exp(-i\varphi/2)]^T/\sqrt{2}$. When projected onto the low energy fermions, the pairing vertex becomes $\tilde{H}_\Delta = \Delta\chi(\mathbf{k}) c^\dagger(\mathbf{k}) c^\dagger(-\mathbf{k})$, where $\chi(\mathbf{k}) \equiv \xi^\dagger(\mathbf{k})(\mathbf{d}\cdot\boldsymbol{\sigma}) i\sigma^y \xi^*(-\mathbf{k})$. The projective form factors (on the conduction band) for $\tilde{\mathbf{d}} = d\hat{x}, \hat{y}, \hat{z}$ are given by $\chi_x(\theta,\varphi) = -\xi^\dagger_\alpha(\varphi)\sigma^z_{\alpha\beta}\xi^*_\beta(-\varphi)e^{i\theta} = 0$, $\chi_y(\theta,\varphi) = i\xi^\dagger_\alpha(\varphi)\delta_{\alpha\beta}\xi^*_\beta(-\varphi)e^{i\theta} = ie^{i\theta}$, $\chi_z(\theta,\varphi) = -\xi^\dagger_\alpha(\varphi)\sigma^x_{\alpha\beta}\xi^*_\beta(-\varphi)e^{i\theta} = -\cos\varphi\, e^{i\theta}$. From this we see that in the odd-parity channel, the only order that fully gaps the FS is the one with $\tilde{\mathbf{d}} = d\hat{y}$, while for $\tilde{\mathbf{d}} = d\hat{x}, d\hat{z}$ the SC order parameter either has no FS component, or leaves a nodal line. This is consistent with Ref. [15], which pointed out that $\tilde{\mathbf{d}} = d\hat{y}$ is the only odd-parity channel to be fully gapped and to involve only intraband pairing. Since interband pairing does not contribute to the pairing instability at weak coupling, and since condensation energy is maximized by a full gap, the $d\hat{y}$ state is expected to be the leading odd-parity instability—as confirmed by detailed renormalization group calculations in Ref. [16]. Or course, odd-parity superconductivity needs to be "seeded" by a bare attraction in an odd angular momentum channel (which could come, e.g., from the Kohn-Luttinger mechanism [27,28]).

We also consider the SC order in the conventional s-wave channel, which couples to fermions via $H^s_\Delta = \bar{\Delta}\psi^\dagger(\mathbf{k}) i\sigma^y (\psi^\dagger)^T(-\mathbf{k})$. Its projective form factor can be obtained by

$$\chi_s(\varphi) = i\xi^\dagger_\alpha(\varphi)\sigma^y_{\alpha\beta}\xi^*_\beta(-\varphi) = -i\sin\varphi. \tag{3}$$

Thus in the s-wave superconducting states there are *two* nodal lines at $\varphi = 0$ and $\varphi = \pi$ [see Fig. 2(a)]. The existence of the two nodal lines tends to strongly suppress T_c for even-parity order. However, attractive interactions in the even-parity channel can be generated by more conventional mechanisms (e.g., phonons), and thus we will discuss s-wave order, too. Note that s- and p-wave orders do not couple because they transform differently under π rotations in the xy plane, and also have opposite mirror eigenvalues (where mirror symmetry is generated in the projected model by $\varphi \to -\varphi$ and in the full model by $k_z \to -k_z$ and conjugation by σ_1). A full comparative analysis of the respective T_c's in the different channels requires a detailed knowledge of microscopic interactions, which is beyond the scope of the current work.

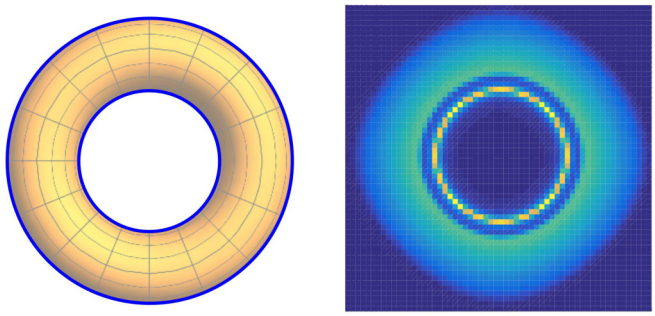

(a) (b)

FIG. 2. (a) The line node of the s-wave state shown on the torus FS (in blue), which corresponds to $\varphi = \pi/2$ and $\varphi = 3\pi/2$. (b) Simulation of the ARPES data of the surface states, showing the coexistence of the Majorana flat band and the drumhead FS. The color code denotes the surface fermionic spectral weight at zero energy, given by $\mathrm{Im}\, G(\omega = 0, \mathbf{k}_{xy}, z = 0)$.

Surface SC. We now turn to surface SC. For a Weyl loop band structure, there exist "drumhead" bands localized on the 2D surface. Unlike true 2D energy bands, these do not extend over the full surface BZ, but are confined in a momentum range given by the projection of the bulk line node. The drumhead bands can be obtained by treating the Hamiltonian (1) at any given (k_x, k_y) point as a one-dimensional subsystem along the z direction, and computing its end states. Recall that the Wilson loop around a point on the line node has a Berry phase of π (since the spin winds by 2π). One can deform the Wilson loop into two paths in the z direction across the BZ, which correspond to the polarizations for two 1D subsystems inside and outside the line node. The π Berry phase around the original Wilson loop indicates that the polarization of the two subsystems differs by $eL/2$ [29,30] (L is the system size), indicating degenerate end states for subsystems either inside or outside the line node. For our model, we compute the surface states using open boundary conditions in the z direction [29,31,32]. We can effectively treat the physical surface as an interface with a trivial insulator with $H = M_0\sigma^x$, where $M_0 > 0$. The surface states are given by $\sigma^z\Psi = \pm\Psi$ for the top and bottom surface, respectively. The two surface states are degenerate, and their dispersion is given by $E = -\mu$.

For our purposes it is interesting to allow for a dispersion in the last term of Eq. (1), i.e., $\mu = \mu(k_x, k_y)$ (which has the same rotation symmetry in the xy plane as the bulk). In this case the drumhead band can have a Fermi surface of its own. For a small dispersion in μ, the density of states on the surface is large, and the surface bands are also unstable towards SC in the presence of interactions [21]. However, since the low energy fermions

are fully spin polarized, s-wave order cannot develop. Thus the drumhead band is immune to an external proximity effect from an s-wave SC. In contrast, in the bulk projection onto one band generates a spin texture, so bulk s-wave pairing is allowed. In the event of bulk s-wave pairing, the drumhead band remains gapless. However, the existence of two new nodal lines in the bulk band structure coming from the SC order induces a new *flat* band [33] on each surface, which cannot disperse, because of particle-hole symmetry in Nambu space. This flat band can again be viewed as a result of π Berry flux around each nodal line [34], similar to the drumhead band. This band is formed by charge-neutral Majorana fermions, and can be viewed as the stacking of Majorana end states from 1D topological superconductors. We show in Fig. 2(b) the simulation of surface angle-resolved photoemission spectroscopy (ARPES) data (momentum distribution curves at energy $\epsilon = 0$), where both the Majorana flat band and the gapless drumhead FS are clearly visible.

We now discuss odd-parity bulk superconductivity in the $\tilde{\mathbf{d}} = d\hat{y}$ channel that fully gaps out the bulk. The SC form factor on the top surface is given by $\chi_y^s(\theta,\varphi) = i(\xi^s)^\dagger(\xi^s)^* e^{i\theta} = ie^{i\theta}$, where $\xi^s \equiv (1,0)^T$ is the spinor structure for the top surface state. From this, we find that the *same* superconducting order that fully gaps out the bulk also fully gaps the surface states with $p+ip$ symmetry. Even for cases where the surface band does not cross the chemical potential, the surface becomes superconducting due to a proximity effect from the bulk. However, the band structure of the surface states is not strongly modified since they are below or above the Fermi level. In Ref. [34] we also present results for the other (subleading) chiral SC states.

Topology of chiral surface SC state. We now address the topological properties of the chiral state $\mathbf{d} = de^{i\theta}\hat{y}$, for which both the bulk and the surface are fully gapped. The topological properties of the bulk SC state has been analyzed in Ref. [15], which used a homotopy argument to identify this state as a "meron superconductor." Here, we concentrate on the surface, which is a $p+ip$ pairing state. Such a state has been proposed for the quantum Hall state at $\nu = \frac{5}{2}$ [23,24] and for the unconventional superconductor Sr_2RuO_4 [35–37]. In the Bogoliubov–de Gennes (BdG) Hamiltonian of a 2D $p+ip$ SC, one can define a homotopy group $\pi_2(S^2)$ from the 2D Brillouin zone to the Nambu spinor space, whose z component is the normal part of the Hamiltonian. At TR invariant points of the BZ, the superconducting order parameter vanishes by fermionic statistics, and the Nambu spinor at these points is forced to point toward the north or south pole. Thus the winding (Chern) number is 1 if the BZ covers both poles, and is 0 if it only covers one pole. The nontrivial case with Chern number 1 corresponds to the case where the normal state has a Fermi surface, also known as the weak phase because the SC in this case is a weak-coupling instability in 2D. As a consequence of the topology, in the weak phase, it is well known that there exist MZMs bound at the core of a vortex of the pairing order parameter. The trivial strong phase, without a Fermi surface, requires a strong interaction to become paired on its own, and hence the name. To deform the strong phase Hamiltonian to the weak phase, the normal state energy $\epsilon(\mathbf{k}=0)$ changes sign, and the gap closes in this process [see Fig. 3(a)], signifying a change in topology.

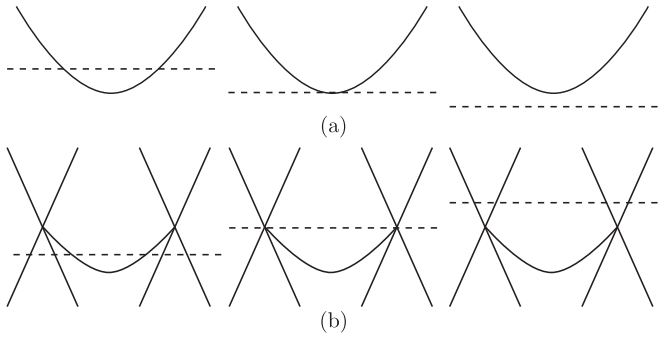

FIG. 3. (a) A process to deform the weak pairing phase into strong pairing phase in 2D $p+ip$ SC, where the dashed lines are the chemical potential. It necessarily involves a gap closing at $\mathbf{k}=0$, where the SC order parameter is forced to vanish by fermionic statistics. (b) The corresponding process for the drumhead surface SC, shown at a given θ. No gap closing is involved with SC order turned on. In the last figure the drumhead dispersion can be further distorted.

For the surface SC states in our case, we *cannot* define the homotopy $\pi_2(S^2)$, because the surface bands do not traverse the full Brillouin zone. Despite the lack of a well-defined topological invariant, we can establish an analogy with the 2D $p+ip$ state. At first glance, it is tempting to classify the case with a surface FS as topological and the case without a surface FS as trivial. However, a careful examination of the band structure reveals that the "weak case" *can* in fact be continuously deformed into the "strong case" (note that despite the name, the SC order is from a weak-coupling instability in the bulk) without closing the gap. We illustrate such a process in Fig. 4(b). This implies these two cases are topologically equivalent and for both there should exist MZMs when vortex lines enter and exit the bulk [38]. However, the above analysis does not include the vortex line, which traps bound states. These vortex line states form a 1D band with a "minigap." If the minigap closes during this process, then this could eliminate the MZMs (see, e.g., Ref. [39]). We show in Ref. [34] that for our case the minigap remains *open*.

To see how to obtain the MZM, we first look at a 2D $p+ip$ SC. We approximate the lattice model with a Dirac fermion at the Γ point, $h = \Delta(k_x\tau^x + k_y\tau^y) - \mu\tau^z$, where the τ matrices are in Nambu space and Δ is the SC order parameter, which has a vortex configuration. However, at this level, there is no distinction between the weak and strong phases. Moreover, the wave function for the bound state diverges as $r \to 0$. A closer look shows that in the vortex core $r \sim 0$ the system is in the normal state, and the wave function at such a short distance depends on the large momentum behavior of $\epsilon(\mathbf{k})$, which is different for the weak and strong phases. One can then show that only for the dispersion of the weak phase can the wave function at small and large r can be matched smoothly [34,40].

However, the situation is different for our case. The surface drumhead band is not a standalone 2D system, and it only exists in a small momentum range around a TR invariant point. In the absence of large momentum states in the surface band, all the surface state wave functions are "smoothed out" at short distances, eliminating the singularity at $r = 0$ [34]. As a result, the surface SC should be topological with vortex core MZMs

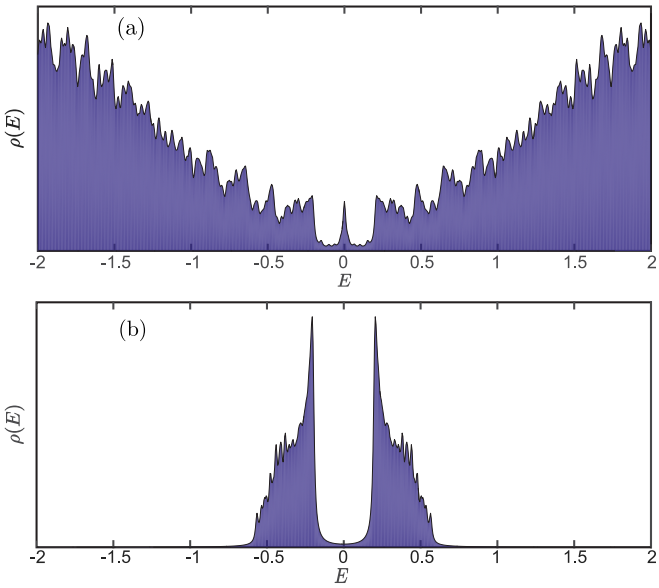

FIG. 4. The density of state plots for a Weyl loop chiral superconductor [(a)] and a 2D $p + ip$ SC with a flat band dispersion [(b)], both in the "strong" pairing phase and with a vortex configuration. The spikes at high energies are due to finite-size effects (the system size is $20 \times 20 \times 10$ for four bands). For both Hamiltonians, there exists a bulk gap at $\mu = 0.2$ (in units of hopping parameters), however, the clear distinction is that there exist in-gap states for the Weyl loop surface SC.

independent of the drumhead band dispersion [41]. To check this logic, we numerically solved and compared the energy spectrum for a Weyl loop SC and 2D $p + ip$ SC, both in the "strong" phase, and we found that only in the former case do there exist an in-gap modes with the wave function peaked at the vortex. In Fig. 4 we show the comparative density of state plots indicating that surface SC in the doped Weyl loop semimetal is topological (in the sense that vortices trap MZM when they enter/exit the bulk) even when the drumhead lies entirely above/below the chemical potential. We also verified that the same results hold for the weak phase of the Weyl loop SC.

In conclusion, we have shown that a doped Weyl loop material hosts entirely new types of topological surface superconductivity. For the fully gapped chiral SC state the surface surface traps MZM when vortex lines enter/exit the bulk, *independent* of the drumhead dispersion. Even for a "conventional" s-wave state, there exists a flat band of neutral Majorana bound states on each surface at the projected location of the FS. Finally, note that while Ca_3P_2 [10], CaAgP, and CaAgAs [12] materials have a fourfold degenerate nodal line (i.e., a Dirac loop), our conclusion can be generalized to these materials. The only difference is that a chiral Dirac loop SC (two copies of Weyl loop SC) should host a single MZM as a *half vortex* line enters and exits the bulk, where only one of the Weyl loop SC copy has a phase winding [42].

We acknowledge useful discussions with T. Kvorning, L. Santos, M. Stone, and C. Wang. We also thank Yang-Zhi Chou, Shouvik Sur, and especially Titus Neupert for feedback on the manuscript. This work was supported by the Gordon and Betty Moore Foundation's EPiQS Initiative through Grant No. GBMF4305 at the University of Illinois (Y.W.). Y.W. acknowledges support by the 2016 Boulder Summer School for Condensed Matter and Materials Physics through NSF Grant No. DMR-13001648, where the initial ideas of this project were conceived.

[1] J.-M. Carter, V. V. Shankar, M. A. Zeb, and H.-Y. Kee, Phys. Rev. B **85**, 115105 (2012).
[2] Y. Chen, Y.-M. Lu, and H.-Y. Kee, Nat. Commun. **6**, 6593 (2015).
[3] R. Schaffer, E. K.-H. Lee, Y.-M. Lu, and Y. B. Kim, Phys. Rev. Lett. **114**, 116803 (2015).
[4] Y. Kim, B. J. Wieder, C. L. Kane, and A. M. Rappe, Phys. Rev. Lett. **115**, 036806 (2015).
[5] K. Mullen, B. Uchoa, and D. T. Glatzhofer, Phys. Rev. Lett. **115**, 026403 (2015).
[6] M. Zeng, C. Fang, G. Chang, Y.-A. Chen, T. Hsieh, A. Bansil, H. Lin, and L. Fu, arXiv:1504.03492.
[7] H. Weng, C. Fang, Z. Fang, B. A. Bernevig, and X. Dai, Phys. Rev. X **5**, 011029 (2015).
[8] R. Yu, H. Weng, Z. Fang, X. Dai, and X. Hu, Phys. Rev. Lett. **115**, 036807 (2015).
[9] A. Yamakage, Y. Yamakawa, Y. Tanaka, and Y. Okamoto, J. Phys. Soc. Jpn. **85**, 013708 (2016).
[10] L. S. Xie, L. M. Schoop, E. M. Seibel, Q. D. Gibson, W. Xie, and R. J. Cava, APL Mater. **3**, 083602 (2015), .
[11] G. Bian, T.-R. Chang, H. Zheng, S. Velury, S.-Y. Xu, T. Neupert, C.-K. Chiu, S.-M. Huang, D. S. Sanchez, I. Belopolski, N. Alidoust, P.-J. Chen, G. Chang, A. Bansil, H.-T. Jeng, H. Lin, and M. Z. Hasan, Phys. Rev. B **93**, 121113 (2016).
[12] Y. Okamoto, T. Inohara, A. Yamakage, Y. Yamakawa, and K. Takenaka, J. Phys. Soc. Jpn. **85**, 123701 (2016), .
[13] J.-W. Rhim and Y. B. Kim, Phys. Rev. B **92**, 045126 (2015).
[14] J. Liu and L. Balents, arXiv:1609.05529.
[15] R. Nandkishore, Phys. Rev. B **93**, 020506 (2016).
[16] S. Sur and R. Nandkishore, New J. Phys. **18**, 115006 (2016).
[17] A. A. Burkov, M. D. Hook, and L. Balents, Phys. Rev. B **84**, 235126 (2011).
[18] Y. X. Zhao and Z. D. Wang, Phys. Rev. Lett. **110**, 240404 (2013).
[19] S. Matsuura, P.-Y. Chang, A. P. Schnyder, and S. Ryu, New J. Phys. **15**, 065001 (2013).
[20] C.-K. Chiu, J. C. Y. Teo, A. P. Schnyder, and S. Ryu, Rev. Mod. Phys. **88**, 035005 (2016).
[21] N. B. Kopnin, T. T. Heikkilä, and G. E. Volovik, Phys. Rev. B **83**, 220503 (2011).
[22] See, however, Ref. [43] for a discussion of the proximity effects in Dirac loop materials, which differ from the Weyl loop materials discussed here by possessing an additional spin degeneracy.
[23] G. Moore and N. Read, Nucl. Phys. B **360**, 362 (1991).
[24] N. Read and D. Green, Phys. Rev. B **61**, 10267 (2000).

[25] L. Fu and C. L. Kane, Phys. Rev. Lett. **100**, 096407 (2008).
[26] Y. Wang and P. Ye, Phys. Rev. B **94**, 075115 (2016).
[27] W. Kohn and J. M. Luttinger, Phys. Rev. Lett. **15**, 524 (1965).
[28] R. Nandkishore, R. Thomale, and A. V. Chubukov, Phys. Rev. B **89**, 144501 (2014).
[29] W. P. Su, J. R. Schrieffer, and A. J. Heeger, Phys. Rev. Lett. **42**, 1698 (1979).
[30] S. T. Ramamurthy and T. L. Hughes, arXiv:1508.01205.
[31] R. Jackiw and C. Rebbi, Phys. Rev. D **13**, 3398 (1976).
[32] I. Martin, Y. M. Blanter, and A. F. Morpurgo, Phys. Rev. Lett. **100**, 036804 (2008).
[33] B. Lu, K. Yada, M. Sato, and Y. Tanaka, Phys. Rev. Lett. **114**, 096804 (2015).
[34] See Supplemental Material at http://link.aps.org/supplemental/10.1103/PhysRevB.95.060506, which includes Refs. [17,24,30,42,44–47], for more details.
[35] T. M. Rice and M. Sigrist, J. Phys.: Condens. Matter **7**, L643 (1995).
[36] G. Baskaran, Physica B (Amsterdam) **223-224**, 490 (1996).
[37] C. Kallin and J. Berlinsky, Rep. Prog. Phys. **79**, 054502 (2016).
[38] Note that this conclusion would not hold for systems with two nodal lines that span the zone, since in that case the surface "drumhead" would extend to the zone boundary, and the gap must vanish by fermion statistics when the chemical potential is at the zone boundary.
[39] P. Hosur, P. Ghaemi, R. S. K. Mong, and A. Vishwanath, Phys. Rev. Lett. **107**, 097001 (2011).
[40] A. Quelle, C. M. Smith, T. Kvorning, and T. H. Hansson, Phys. Rev. B **94**, 125137 (2016).
[41] Note that, due to the large density of states on the drumhead band, it is entirely possible that the surface band becomes superconducting at a higher temperature than the bulk does. However, in this case the MZM on the top and bottom surface can couple through the gapless bulk.
[42] D. A. Ivanov, Phys. Rev. Lett. **86**, 268 (2001).
[43] B. Roy, arXiv:1607.07867.
[44] A. Y. Kitaev, Phys. Usp. **44**, 131 (2001).
[45] J. Alicea, Rep. Prog. Phys. **75**, 076501 (2012).
[46] B. A. Bernevig and T. L. Hughes, *Topological Insulators and Topological Superconductors* (Princeton University Press, Princeton, NJ, 2013).
[47] Y. Nishida, L. Santos, and C. Chamon, Phys. Rev. B **82**, 144513 (2010).